Supporting Information

For *Dalton Transactions*

Approaching the Size Limit of Organometallic Layers: Synthesis and Characterization of Highly Ordered Silver-Thiolate Lamellae with Ultra-short Chain Lengths

Zichao Ye,[a,b] Lito P. de la Rama,[a,b] Mikhail Y. Efremov,[c] Jian-Min Zuo,[a] and Leslie H. Allen*[a,b]

[a] Department of Materials Science and Engineering, Frederick-Seitz Materials Research Laboratory, University of Illinois at Urbana-Champaign, Urbana, Illinois 61801, United States

[b] Coordinated Science Laboratory, University of Illinois at Urbana-Champaign, Urbana, Illinois 61801, United States

[c] College of Engineering, University of Wisconsin-Madison, Madison, Wisconsin 53706, United States

* Leslie H. Allen (l-allen9@illinois.edu)

Elemental analysis of thiolate composition

Table SI-I. Mass fractions of each element in AgSCn (n=1-16)

	Ag%		S%		C%		H%	
	Measured	Calculated	Measured	Calculated	Measured	Calculated	Measured	Calculated
AgSC1	68.22	69.61	21.09	20.69	7.39	7.75	1.76	1.95
AgSC2	62.78	63.83	18.27	18.97	14.17	14.21	2.89	2.98
AgSC3	59.88	58.94	17.94	17.52	19.58	19.69	3.73	3.85
AgSC4	53.94	54.74	17.57	16.27	24.28	24.38	4.45	4.60
AgSC5	48.92	51.10	15.51	15.19	28.23	28.45	5.22	5.25
AgSC6	46.69	47.92	13.82	14.24	31.72	32.01	5.65	5.82
AgSC7	43.78	45.11	13.59	13.41	34.90	35.16	6.33	6.32
AgSC8	43.83	42.61	12.50	12.67	37.81	37.96	6.70	6.77
AgSC9	37.69	40.37	11.05	12.00	40.33	40.46	7.31	7.17
AgSC10	39.72	38.36	11.29	11.40	42.50	42.71	7.43	7.53
AgSC11	35.94	36.54	11.31	10.86	44.38	44.75	7.77	7.85
AgSC12	34.34	34.88	10.19	10.37	46.47	46.60	8.15	8.15
AgSC14	33.63	31.98	10.26	9.51	49.65	49.85	8.70	8.67
AgSC15	30.57	30.70	9.49	9.13	51.05	51.28	8.93	8.89
AgSC16	28.81	29.52	8.71	8.78	52.39	52.60	9.13	9.10

*The measured percentages are compared with the theoretical percentages calculated from molecular weight.

Morphology of AgSCn (n=8-16): SEM imaging

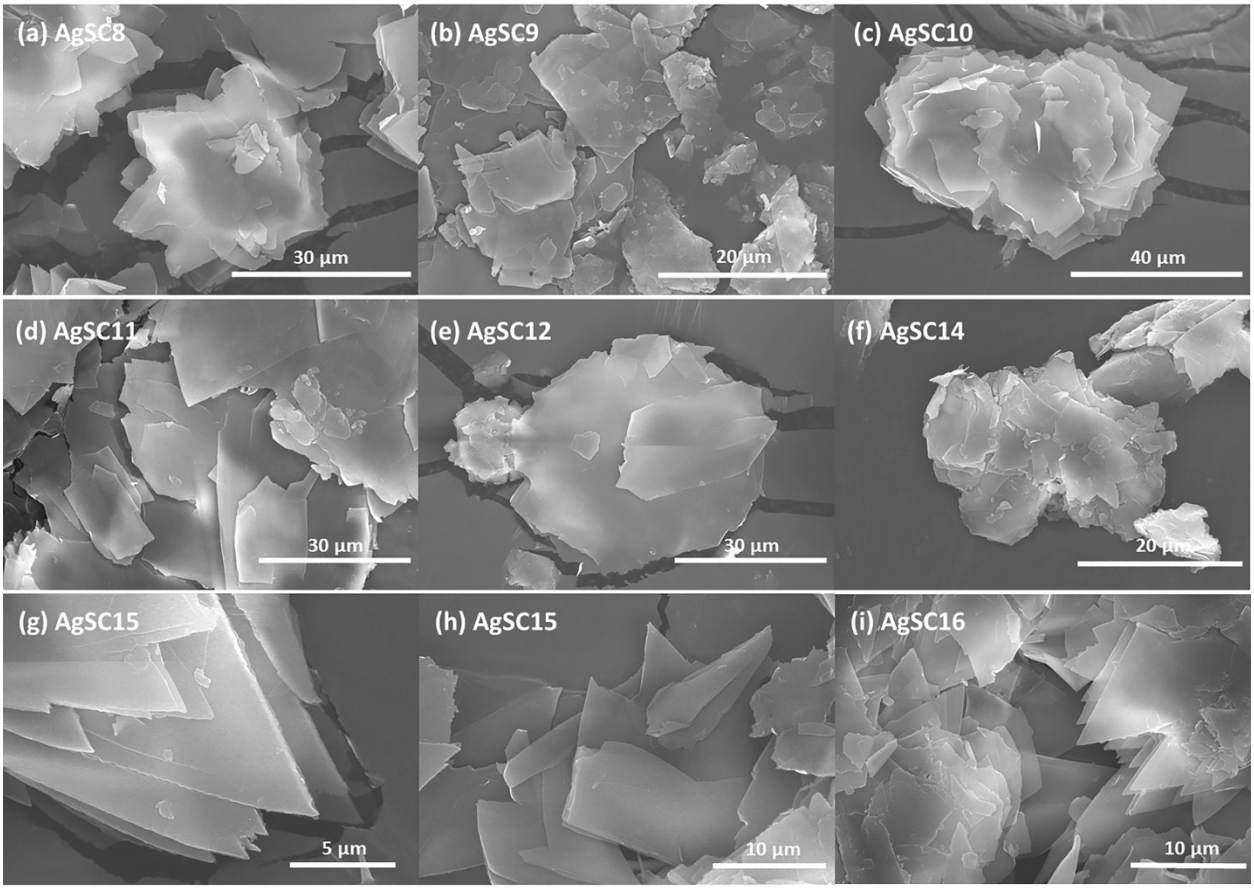

Figure SI-1. SEM images of AgSCn (n=8-16) crystals: all samples show well-defined nanosheet-shaped lamellar morphology.

XRD patterns of as-synthesized vs. recrystallized or Ostwald ripened AgSCn

Table SI-II. comparison of XRD (0k0) diffractions between the as-synthesized and recrystallized (AgSC7) or Ostwald ripened (AgSC3) crystals, in terms of peak FWHM, peak integrated intensity and number of peaks.

	AgSC7		AgSC3	
	Synthesized	Recrystallized	Synthesized	Ostwald Ripened
Sample Mass (mg)	11.7	7.0	22.0	13.9
FWHM	0.21°	0.19°	0.21°	0.16°
Normalized I(010)*	1.0	17.9	1.0	1.6
# of Peaks	5	14	3	6

*The normalized integrated intensity of I(010) peak for as-synthesized samples are set to be 1.0.

XRD patterns of AgSCn (n=6-16)

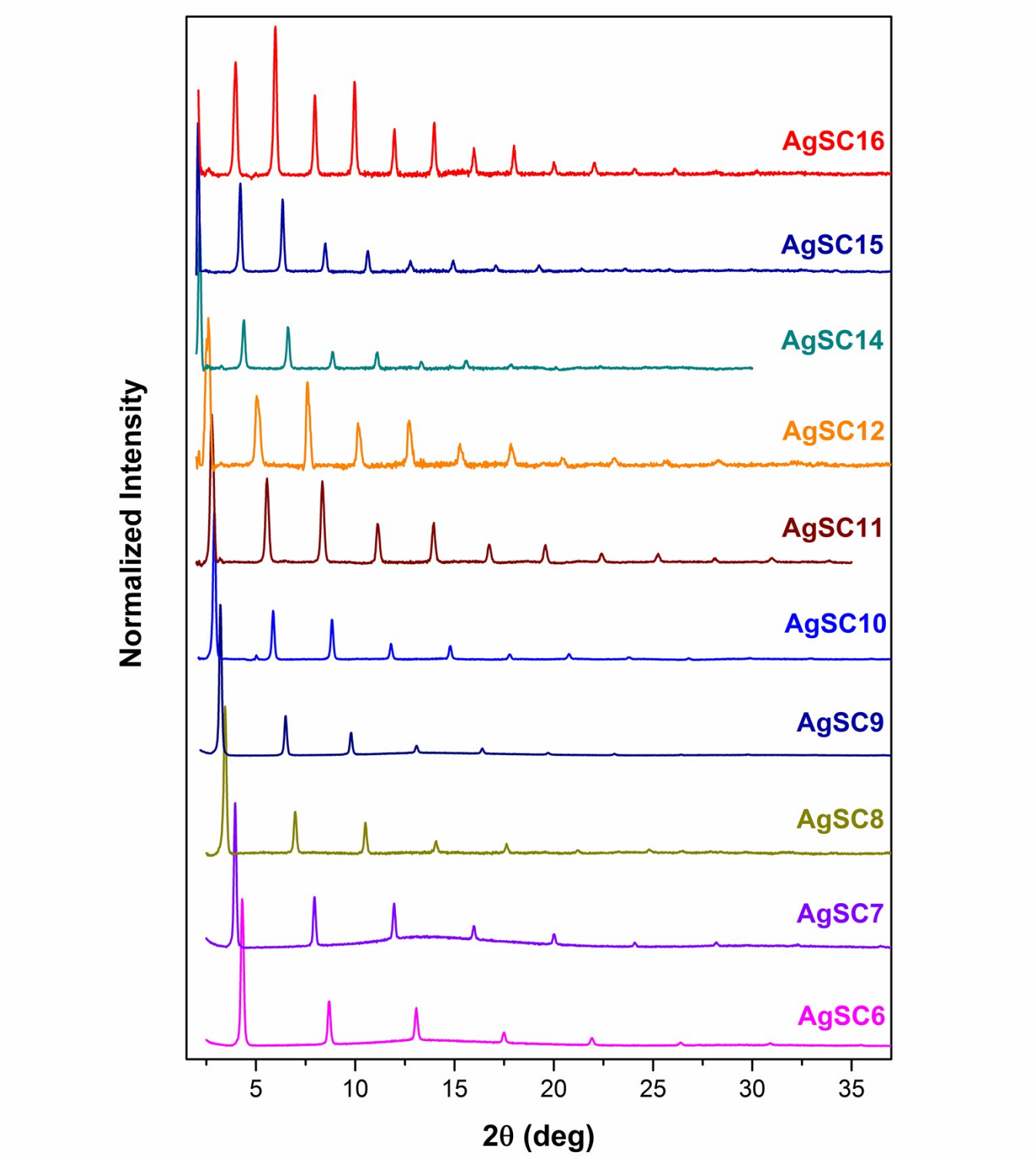

Figure SI-2. Plot shows the raw data of XRD (0k0) lamellar reflections for AgSCn (n=6-16) crystals.

XRD measurement on the residues of decomposed AgSC3

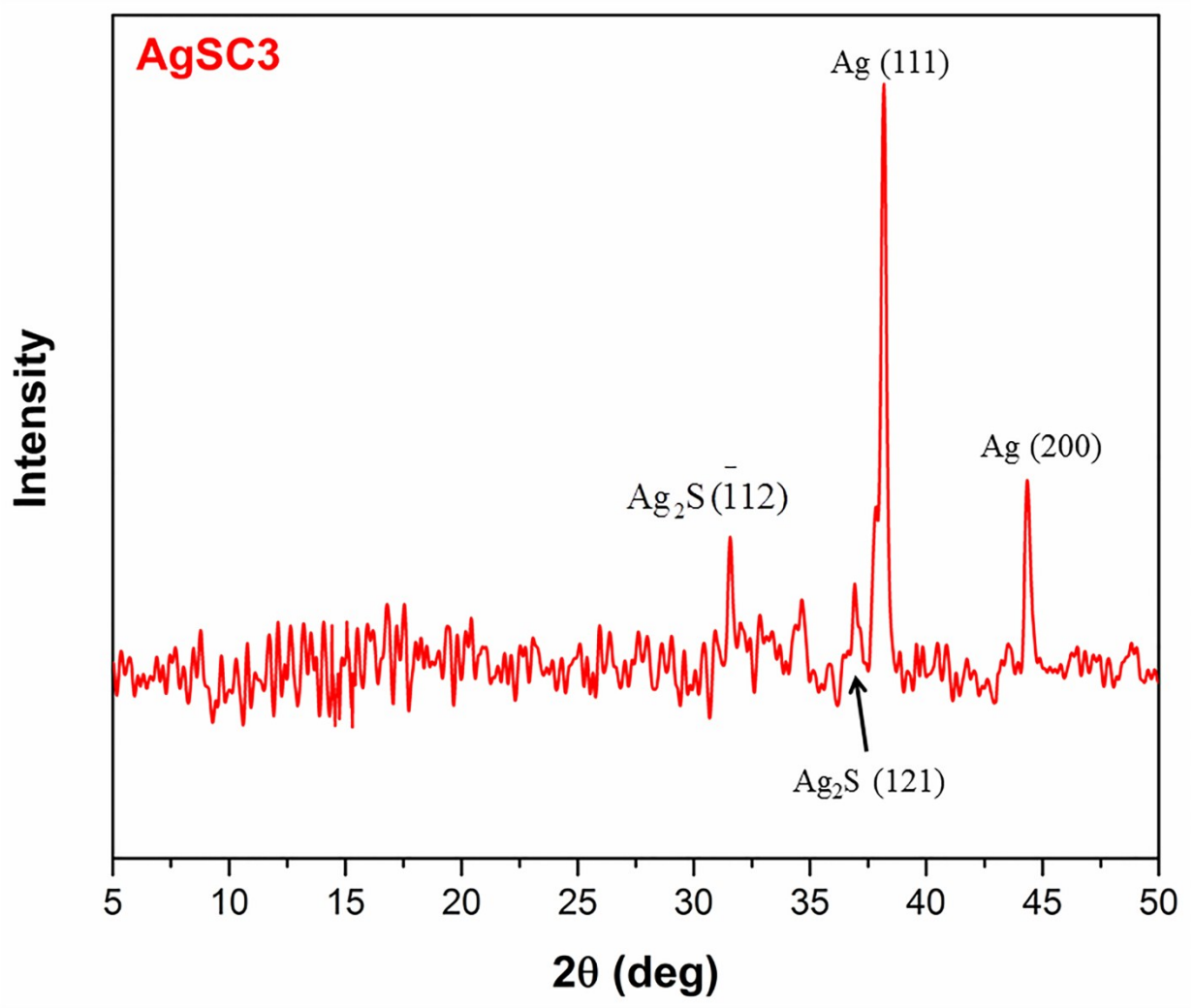

Figure SI-3. XRD pattern of residue materials after the decomposition of AgSC3. Reflection peaks of Ag (111), Ag (200), Ag_2S ($\bar{1}12$) and Ag_2S (121) are observed.

DSC traces of Ag_2S

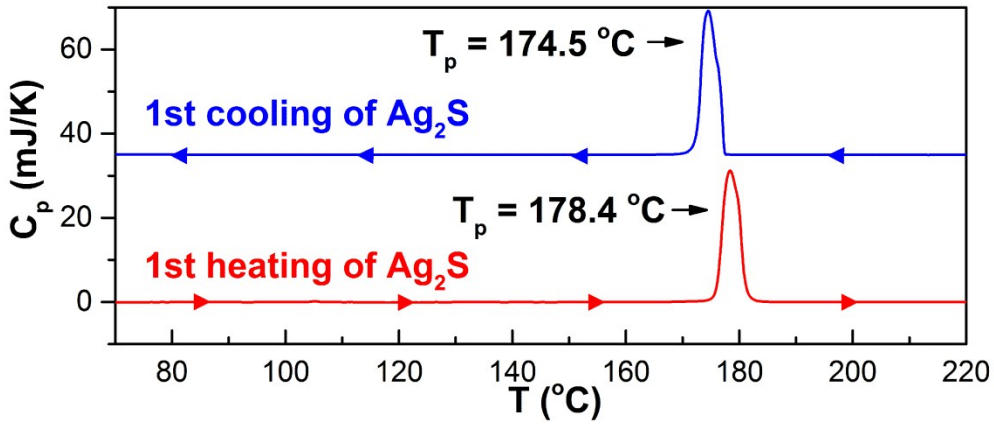

Figure SI-4. DSC traces of commercial Ag_2S with 10 °C/min scanning rate.

Vibration modes of hydrocarbon groups (FTIR analysis)

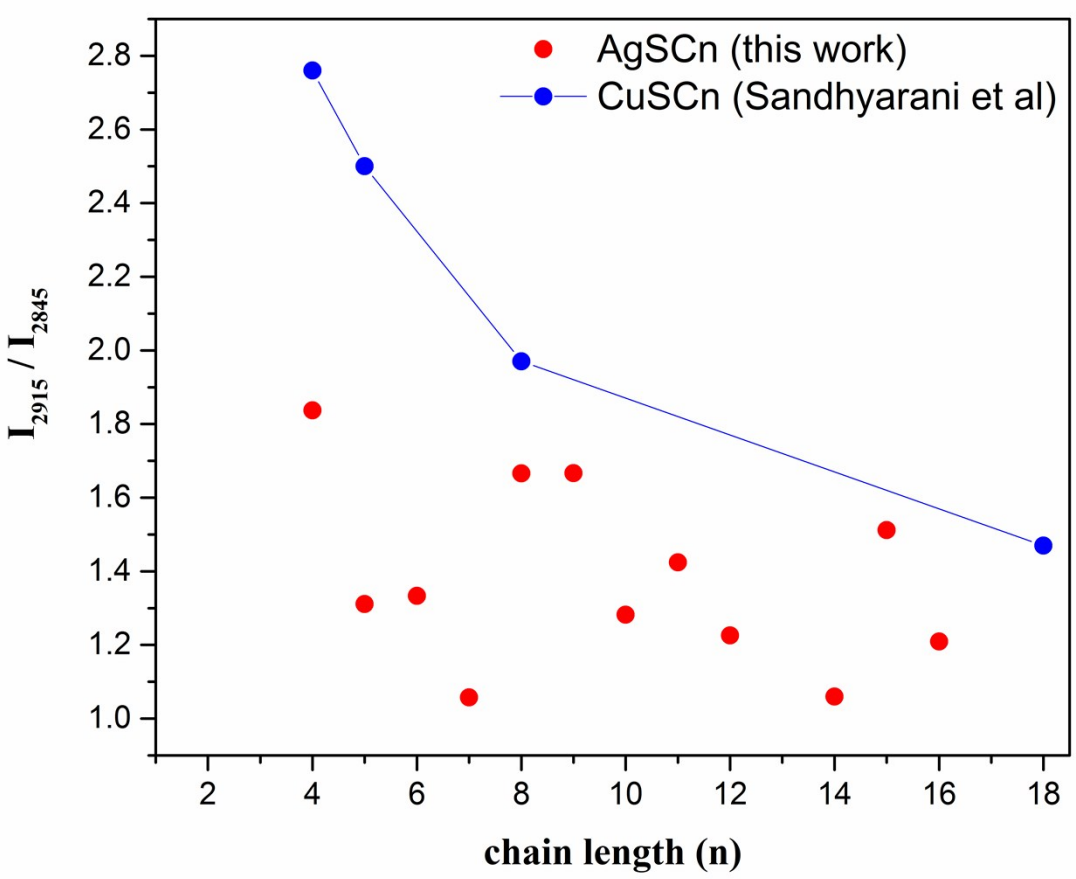

Figure SI-5. Plot shows the area intensity ratio between d^- and d^+ FTIR peaks for AgSCn (n=4-16) and CuSCn (n=4, 5, 8, 18). The data of CuSCn in this plot are replotted from the work of Sandhyarani et al.[1]

In Figure 7a (main text), two distinct peaks observed at 2860-2875 cm^{-1} and 2950-2960 cm^{-1} are assigned to the symmetric (r^+) and asymmetric (r^-) stretching modes of terminal CH_3 groups of AgSCn, respectively.[1-4] The intensity of these peaks relative to that of d^+ and d^- modes reduces as chain length increases, due to the decreasing percentages of CH_3 groups. The r^+ peaks are almost buried in the shoulder of d^+ peaks for n>7. AgSC1 only shows one major signal at 2889 cm^{-1}, which is suggested as the CH_3 symmetric stretching peak

(r^+). A similar peak is observed for methanethiol absorbed on Ag surface at 2908 cm^{-1}, which is 40 cm^{-1} red-shifted from that of CH_3SH.[5]

Table SI-III lists the peak locations of all C-H stretching modes for the AgSCn (n=1-16) studied in this work.

Table SI-III. C-H stretching modes of AgSCn (n=1-16) (unit: cm^{-1})

n	$\nu_s(CH_2)$, d^+	$\nu_{as}(CH_2)$, d^-	$\nu s(CH_3)$, r^+	$\nu_{as}(CH_3)$, r^-
1	-	-	2889	2960
2	-	2917	2861	2950
3	-	2923	2863	2953
4	2850	2920	2870	2955
5	2847	2916	2868	2952
6	2847	2916	2871	2954
7	2845	2915	2870	2953
8	2846	2916	2872	2953
9	2846	2915	2871	2953
10	2846	2915	2872	2954
11	2846	2915	2872	2953
12	2845	2915	2873	2953
14	2845	2913	2872	2952
15	2846	2915	2872	2953
16	2847	2916	2873	2952

Degradation of AgSC15 lamellae under e-beam exposure

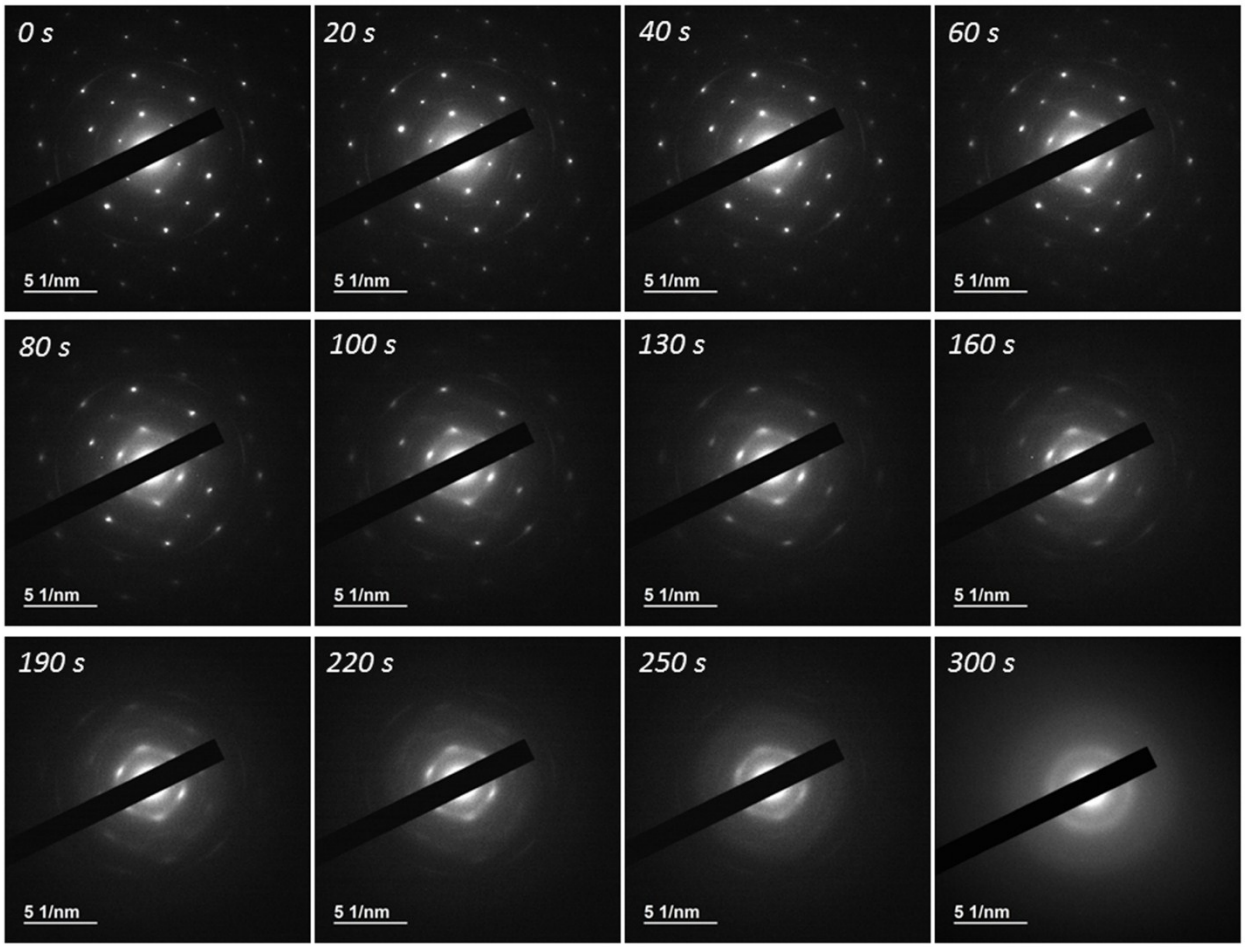

Figure SI-6. Images show the evolution of SAED patterns (zone axis: [010]) of AgSC15 lamellae under e-beam exposure. The well-defined single crystal degrades into amorphous within 5 min.

Molecular structure and van der Waals gap of odd and even AgSCn

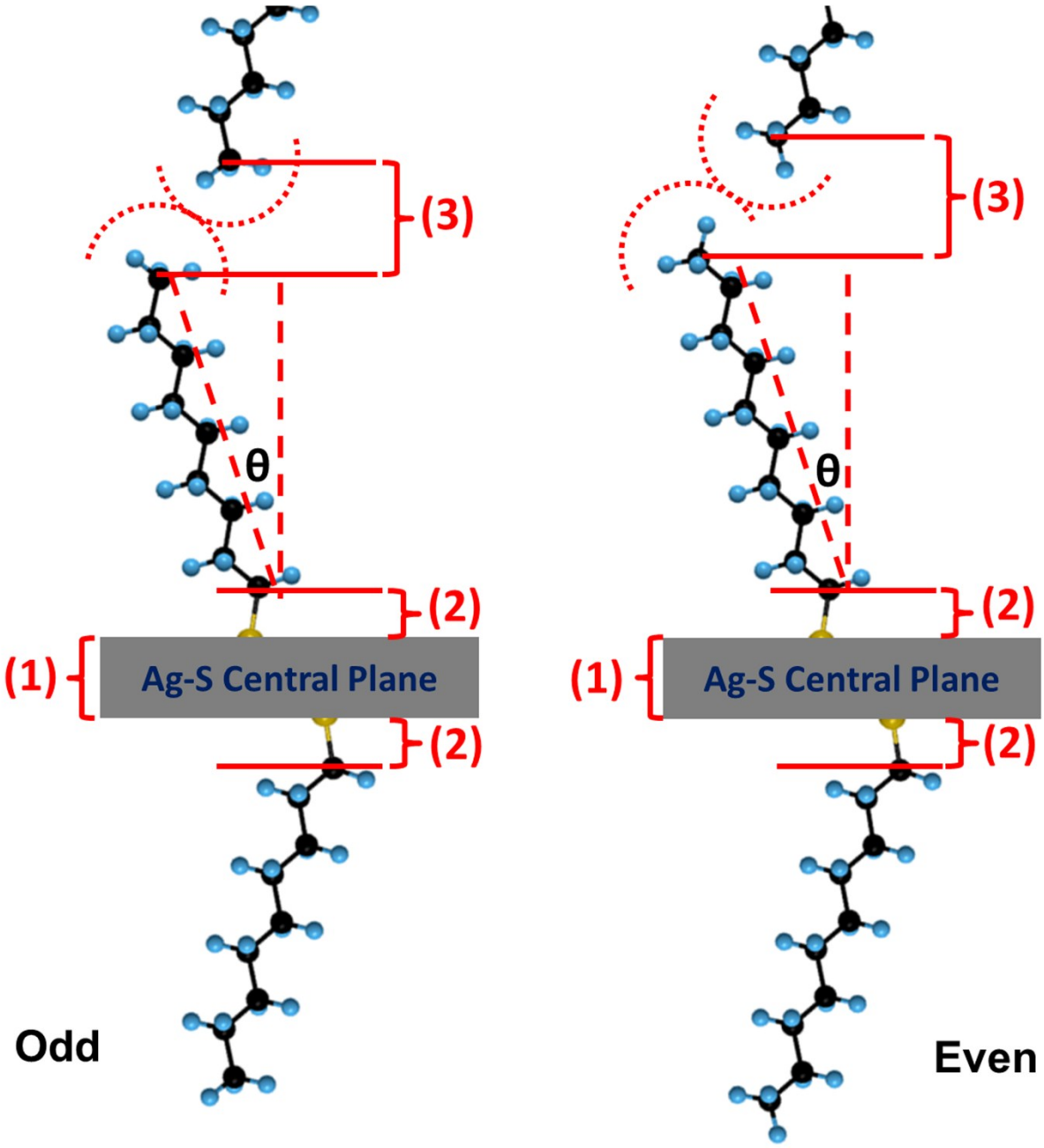

Figure SI-7. Schematics show the molecular structures of odd and even AgSCn. The intercepts of fittings in Figure 10a represent the sum of (1) Ag-S central plane thickness, (2) twice the projection of S-C bond length along [0k0] direction, and (3) the interlayer van der Waals gaps. The tilt angle of the chains is about 18°.

References

1. N. Sandhyarani and T. Pradeep, *J. Mater. Chem.*, 2001, **11**, 1294-1299.
2. A. N. Parikh, S. D. Gillmor, J. D. Beers, K. M. Beardmore, R. W. Cutts and B. I. Swanson, *The Journal of Physical Chemistry B*, 1999, **103**, 2850-2861.
3. S.-H. Park and C. E. Lee, *Chem. Mater.*, 2006, **18**, 981-987.
4. P. N. Nelson and H. A. Ellis, *Dalton Trans.*, 2012, **41**, 2632-2638.
5. S. B. Lee, K. Kim, M. S. Kim, W. S. Oh and Y. S. Lee, *J. Mol. Struct.*, 1993, **296**, 5-13.